Effect of imperfections on the actuation stiffness of the Kagome Double Layer Grid

D. D. Symons[a], J. Shieh[b], N. A. Fleck[a]

[a] Cambridge University Engineering Department, Trumpington Street,
Cambridge, CB2 1PZ, UK

[b] Department of Materials Science and Engineering, National Taiwan University,
1 Roosevelt Road, Sec. 4, Taipei, Taiwan

Abstract

The Kagome Double Layer Grid (KDLG) behaves as a plate with high bending stiffness and high membrane stiffness under passive loading, yet can change shape by the extensional actuation of any of its constituent bars: it is a suitable microstructure for a morphing plate. The statically determinate pin-jointed KDLG can be actuated by bar extension, without the storage of energy within the remaining structure. In contrast, the KDLG with rigid joints resists the axial actuation of any bar by the bending of its remaining bars, as quantified by the actuation stiffness of the structure. The actuation stiffness of a set of steel KDLG structures with brazed joints is measured experimentally and compared with predictions by the finite element method. The predicted actuation stiffnesses for the perfect KDLGs much exceed the measured values, and it is argued that the low values of observed actuation stiffness are due to the presence of geometric imperfections introduced during manufacture. In order to assess the significance of geometric defects upon actuation stiffness, finite element calculations are performed on structures with a stochastic dispersion in nodal position from the perfectly periodic arrangement, and on structures with wavy bars. It is found that bar waviness has the dominant effect upon the actuation stiffness. The predicted actuation stiffness for the imperfect structures are in satisfactory agreement with the measured values assuming the same level of imperfection between theory and experiment.

Keywords: B: Elastic-plastic material; Structures; C: Finite elements; Mechanical testing; Morphing structures

1. Introduction

There is much recent interest in the development of morphing materials that are stiff to external loads yet can accommodate large changes in shape upon actuation by lengthening (or shortening) a portion of the material. Hutchinson et al. (2003) have proposed that the planar Kagome truss (Fig.1a) is a suitable two-dimensional microstructure for shape changing (morphing) application. The finite planar Kagome truss, with suitable patch bars on the periphery (Fig. 1b) is both statically and kinematically determinate in its pin-jointed form. Consequently, it is a rigid topology, but becomes a single-degree-of-freedom mechanism if any bar is replaced by an actuator. The Kagome topology has the additional advantage that the elastic, infinite planar Kagome truss is isotropic and has an in-plane modulus which attains the upper Hashin-Shtrikman bound, see Hyun and Torquato (2002). Practical morphing materials have, by necessity, rigid (welded) joints. Wicks and Guest (2003) have shown that the rigid joint 2D Kagome truss provides a low resistance to actuation compared to a fully triangulated planar grid.

The Kagome Double Layer Grid (KDLG) is a sandwich construction comprising two planar Kagome trusses and a double layer tetrahedral core, see Fig. 2a. The KDLG has been proposed by Hutchinson et al. (2003) and Symons et al. (2004) as a suitable microstructure for morphing plate structures. The extensional stiffness and bending stiffness of the KDLG are high due to the fact that it behaves as a sandwich plate with planar Kagome grids as the faces.

The infinite, periodic KDLG is neither statically nor kinematically determinate. However, Symons et al. (2004) have shown that the finite pin-jointed KDLG can be made to be statically and kinematically determinate by two modifications to its geometry. The structure is made asymmetric about its mid-plane (termed the asymmetric KDLG), and is given additional patch bars on its periphery, see Fig. 2b. Consequently, the rigid joint version of this *asymmetric patched KDLG* is a stiff, stretching dominated structure under passive loading. Now consider the removal of any bar from the pin-jointed *asymmetric patched KDLG*; the structure now behaves as a mechanism with a single degree of freedom. The rigid joint version reflects this property: when one or more bars are

elongated by suitable actuators, the rigid joint structure resists this actuation by a compliant deformation mode dominated by bar bending. The deformation mode reduces to an internal collapse mechanism in the pin-jointed limit. Thus, the asymmetric patched KDLG is an attractive topology for a morphing structure.

1.1. Imperfection sensitivity

Practical, as-manufactured structures contain geometric imperfections. These imperfections may influence both the passive and active structural response, and it is the aim of the present study to investigate the sensitivity of the actuation stiffness of the KDLG to imperfections.

The effect of imperfections upon the macroscopic stiffness and strength of a lattice material is dependent upon both the type of imperfection and the mode of deformation exhibited by the perfect pin-jointed parent structure. For example, the fully triangulated 2D lattice (with a connectivity of 6 bars per joint) is a highly redundant stretching structure in pin-jointed form. An imperfection in the form of a random perturbation in position of nodes has only a minor effect upon the overall stiffness and strength. In contrast, an imperfection in the form of waviness of each bar dramatically reduces the macroscopic stiffness and strength due to the large knock-down in axial stiffness and strength of each bar.

The regular hexagonal honeycomb has a different imperfection sensitivity to that of the fully triangulated structure. Under in-plane hydrostatic loading it behaves as a stiff, stretching structure. However, on moving the nodes to form an irregular hexagonal honeycomb, the rigid joint structure deforms in a much more compliant manner by the local bending of bars, see Chen et al. (1999, 2001). Similarly, the introduction of bar waviness degrades the structure from stretching-governed to bending-governed, for macroscopic hydrostatic loading. This behaviour is fundamentally different to that of the regular hexagonal honeycomb under in-plane deviatoric loading. Under deviatoric loading, the perfect structure deforms by bar bending, and the macroscopic stiffness and

strength are relatively insensitive to the geometric defects of bar waviness and nodal position.

In a recent study, Symons et al. (2004) have explored theoretically the actuation response of finite perfect KDLGs. Upon actuation, the structure deforms by a combination of bar bending and stretching, and for such structures the significance of imperfections has not been resolved. In this paper, the predicted sensitivity of actuation stiffness to a random repositioning of nodes and to the degree of bar waviness are compared with measurements of actuation stiffness on fabricated KDLGs.

2. Introduction to the 7-hexagon KDLG

Symons et al. (2004) have studied the effect of the number of repeating unit cells within a pin-jointed KDLG upon the total number of collapse mechanisms and states of self-stress within the structure. They demonstrated that conversion of the infinite, periodic KDLG to a finite form requires the addition of peripheral patch bars in order to remove the collapse mechanisms associated with the reduced connectivity at the periphery. Their analysis of the static determinancy of the patched or unpatched finite structure revealed the existence of states of self-stress, unless the structure has a very limited number of unit cells (less than 7). For example, the symmetric-unpatched structure with 7 hexagons on each face contains a single state of self-stress, see Fig. 3a. Symons et al. (2004) showed that such states of self stress can be removed by breaking the symmetry of the structure about the mid-plane to produce a so-called *asymmetric version* of the KDLG. The 7-hexagon asymmetric-unpatched version is sketched in Fig. 3b.

In the present study, the actuation response of the 7-hexagon KDLG is measured and calculated for versions which are either symmetric (S) or asymmetric (A), and either patched (P) or unpatched (U). These four variants are labelled symmetric-unpatched (S-U), asymmetric-unpatched (A-U), symmetric-patched (S-P), and asymmetric-patched (A-P), and are catalogued in Fig. 3.

2.1. States of self-stress

The single state of self-stress in the S-U KDLG is triggered by the actuation of any bar associated with this state of self-stress. In contrast, the A-U KDLG, as shown in Fig. 3b, contains no states of self-stress, and provides no resistance when any bar is actuated. In rigid joint form, a small resistance to actuation is anticipated due to bending of bars in the A-U grid, and a much larger resistance due to stretching of bars in the S-U grid.

2.2. Patching scheme

The A-U KDLG is statically determinate with no states of self-stress ($s = 0$), but it does contain $m = 30$ collapse mechanisms. To make the structure kinematically determinate ($m = 0$), yet remain statically determinate ($s = 0$), these 30 mechanisms are eliminated by a peripheral patching scheme, as shown in Fig. 3d. This patching scheme is applied to the top layer, mid-plane and bottom layer of the KDLG, with three additional bars.

Now consider the S-U KDLG. It contains a single state of self-stress ($s = 1$) and $m = 31$ mechanisms. The above patching scheme does not remove all mechanisms and the final count of states of self-stress and mechanisms for the symmetric-patched (S-P) grid is $s = 6$, $m = 6$ for the structure sketched in Fig. 3c. The number of mechanisms m and states of self-stress s for each of the above KDLG structures is summarised in Table 1.

Table 1

The four versions of the 7-hexagon KDLG

	Symmetric (S)	Asymmetric (A)
Unpatched (U)	S-U $s = 1$, $m = 31$	A-U $s = 0$, $m = 30$
Patched (P)	S-P $s = 6$, $m = 6$	A-P $s = 0$, $m = 0$

2.3. Actuation of the KDLG

Symons et al. (2004) have explored theoretically the actuation response of the four variants of the 7-hexagon KDLG by replacing one bar with an axial actuator. They considered rigid-jointed structures and determined the sensitivity of actuation response to the *stockiness S* of the bars, as defined by the ratio of the radius of gyration λ to the length l of the bar,

$$S = \lambda / l \tag{1}$$

The second moment of area I of the bar cross section can be expressed by

$$I = A\lambda^2 \tag{2}$$

in terms of the cross-sectional area A and radius of gyration λ of the bar. Symons et al. (2004) showed that the achievable actuation strain is limited by the elastic buckling and yielding of the bars, and has a maximum value at a stockiness of S = 0.003 to 0.1, depending upon the assumed yield strain of the solid.

3. Manufacture of KDLG structures

A single specimen of each of the four variants of 7-hexagon KDLG shown in Fig. 3 was manufactured by the assembly of two Kagome face sheets and two folded tetrahedral core layers. The struts of the core and faces were laser cut from a low carbon steel sheet using a CNC-controlled machine. The measured elastic-plastic uniaxial response of the steel sheet is given in Fig. 4a, measured at a strain rate of 10^{-3} s^{-1}. The low carbon steel has a measured Young's Modulus E = 200 GPa and a 0.2% offset yield strength of 200 MPa, giving a yield strain of 0.001. The constituent bars of the KDLGs were manufactured to a length of 40.5 mm, a square cross-section of 1 x 1 mm, and thereby a stockiness of S = 0.007. The previous study of Symons et al. (2004) shows that this value of stockiness is close to optimal for maximising the actuation strain, for the given value of yield strain. The two core component sheets were cold pressed by a CNC-controlled folding machine into their three-dimensional form and were then assembled with the face sheets into the KDLG geometry. Two manual operations were used to bond together the

structure: spot welding of the nodes, followed by reinforcement of the nodes by silver soldering with a gas flame and silver solder applied locally to each joint. Fig. 4b shows an example of a completed KDLG specimen: the S-U version.

The core geometry used in the construction of the asymmetric KDLG differs from that used for the symmetric KDLG, see Fig. 2. In the symmetric case, the nodes *on each face* of the folded tetrahedral core layers lie on the same plane, as in Fig. 2a. In the asymmetric case, the mid-plane nodes are perturbed in the through-thickness direction, as shown in Fig. 2b. The amplitude of the asymmetry of the nodes about the mid-plane of the asymmetric KDLG is equal to 14% of the total KDLG depth.

3.1. Measurement of imperfections in fabricated structures

A 3-axis co-ordinate measuring machine[1] was used to measure as-manufactured imperfections in the manufactured KDLG specimens. Imperfections in nodal position were measured in both the through-thickness and in-plane directions. Additionally, the degree of bar waviness was measured by measuring the co-ordinates of each bar at mid-span in relation to its two ends. The degree of imperfection was measured for each variant of KDLG, and was found to show little variation from one type of structure to the next. Consequently, the values of imperfection reported below are averaged over measurements taken on all four variants.

The root mean square (RMS) value of nodal perturbation in the through-thickness direction from that of the perfect structure was measured to be 2.1mm. This imperfection is quite large relative to the bar cross-section of 1 x 1 mm, and is largely ascribed to the manual nature of the spot welding operation during specimen fabrication. The magnitude of the imperfection of nodal location in the plane of the KDLG is defined by the RMS value of the radial displacement of each node from that of the perfect lattice. The measured RMS value of 0.23mm is much less than the out-of-plane value of 2.1mm, and this is ascribed to the fact that the Kagome face sheets were accurately cut by the CNC

[1] An OMICRON A001 machine was used, with a sensor head tip radius of 0.5mm.

laser cutting machine. Finally, the RMS value of the amplitude w_0 of bar waviness was measured to be 0.55 mm.

4. Actuation of the fabricated KDLG structures

4.1. Test protocol

Each of the four KDLG structures was actuated by replacing a single bar of the central hexagon on one of the Kagome face trusses by an instrumented actuator, see Fig. 3. A screw-driven mechanical test machine was used as the actuator: the two nodes of the removed member were stretched apart in a direction parallel to that of the removed bar, using a pair of L-shaped loading fixtures (see Fig. 5). The load was measured using the load cell of the test machine while the displacement of the two loading nodes was measured continuously by a laser extensometer. Five load-unload cycles were applied to each specimen, incrementing the peak load in 10N steps up to a maximum value of 50N, at a displacement rate of 10^{-2} mm s^{-1}.

4.2. Measurements of actuation response

The actuation force versus deflection responses are plotted in Fig. 6a for the two symmetric KDLGs, and in Fig. 6b for the two asymmetric KDLGs. Finite element predictions of the loading response are included to allow comparison; details of the finite element model are given later.

The initial measured stiffness of the structures decreases by a factor of 5 from most stiff to least stiff: S-P, S-U, A-P, A-U. The measurements confirm that a symmetric structure and the presence of patch bars each contribute to the actuation stiffness. The symmetric patched (S-P) structure is essentially linear elastic over the applied load range (up to 50N). However, the less stiff KDLGs show increasing hysteresis with increasing load level in their force-deflection responses, due to plastic deformation within the struts. For example, when the asymmetric unpatched (A-U) structure was loaded up to 50N (and 2.8 mm actuation) the residual deflection was 0.3mm.

5. Predicted actuation response

Actuation of the KDLG structures by extension of the single central bar has been simulated by finite element analysis. Recall that the position of the actuated bar in each 7-hexagon variant is shown in Fig. 3. The actuated bar is removed and pinned displacement constraints are applied so that the relative separation of the end nodes of the replaced bar is prescribed. The axial force between these two end nodes is calculated as a function of nodal separation. No rotational constraints are applied to any nodes other than those required to eliminate rigid body motion.

5.1. Prediction of actuation stiffness

Two commercially available finite element packages were used to calculate the initial actuation stiffness of the structures: Pro/Mechanica (PTC, 2001) and ABAQUS/Standard (HKS, 2003). Both the Pro/Mechanica and ABAQUS simulations assumed linear elastic, infinitesimal displacements in order to calculate the initial actuation stiffness. The struts comprise an isotropic elastic solid of Young's modulus 200 GPa and Poisson ratio 0.3.

Pro/Mechanica uses a p-version of the finite element method. Theoretical foundations of the p-method are given by Babuska et al. (1981) and Babuska and Szabo (1982). The basic idea is that the degree of interpolation function within each element can be adjusted to give any desired convergence accuracy. This method allows for automatic convergence by a multi-pass process: the element order is refined as required to give any desired solution accuracy, here taken to be 1% on actuation stiffness. The constituent bars of the KDLG were treated as single elements. Timoshenko (shear flexible) beams were employed with the joints treated as rigid nodes.

The element order in the ABAQUS program is controlled manually by the user. In the ABAQUS simulations a single "B33" 2-node cubic beam element was used for each strut. The B33 element is an Euler-Bernoulli beam that does not allow for shear deformation. The actuation stiffnesses obtained by the two finite element procedures are compared in Table 2. The differences between the Pro/Mechanica and ABAQUS results are sufficiently small for us to conclude:

(i) shear deformation is insignificant for these structures, and

(ii) the ABAQUS calculations, based on a single element per bar with cubic interpolation, suffice for our purposes.

Table 2

Measured and predicted actuation stiffness of 7-hexagon KDLGs

		S-P	S-U	A-P	A-U
Pro/Mechanica	(N/mm)	174.18	87.46	72.08	21.72
ABAQUS	(N/mm)	174.21	87.48	72.17	21.75
% difference		0.019	0.022	0.12	0.17

5.2. Prediction of non-linear actuation response

The above calculations of actuation stiffness give no information on the effects of finite deformation and material non-linearity upon the response of the perfect structures. Leung et al. (2004) have shown that geometric softening occurs in actuated planar Kagome trusses due to finite deformation effects. It is clear from the observed hysteresis in actuation response that significant plastic deformation occurs in the KDLG structures. In order to determine whether the observed actuation response can be captured by a full non-linear finite element analysis of the perfect structure, ABAQUS predictions of actuation were made for the four KDLG variants, employing both geometric and material non-linearity.

The non-linear calculations were performed with 10 type B33 elements used to model each beam, in order to capture local non-linear effects. The measured elastic-plastic uniaxial response of the steel sheet was employed, recall Fig. 4a, with von Mises plastic flow theory and isotropic hardening. The finite element predictions of the loading and unloading actuation force versus displacement for the four perfect variants, loaded up to

50N, are included in Figs. 6a and 6b. The predictions for the symmetric (S-P and S-U) and the asymmetric-patched (A-P) structures give the same linear response as that obtained by the previous linear finite element analyses as summarised in Table 2. In contrast, the asymmetric-unpatched (A-U) KDLG gives pronounced non-linearity at loads exceeding 30N. The hysteresis present in the predicted response of the A-U structure is due to material non-linearity, and the linear unloading response indicated that finite deformation effects can be ignored.

5.3. Comparison of predicted actuation stiffness for perfect geometry with measured response

The measured initial stiffnesses are compared with finite element (FE) predictions in Table 3 and in Fig. 6. Only in the case of the asymmetric-unpatched (A-U) KDLG does the measured experimental actuation stiffness show good agreement with the FE prediction. The measured stiffness of the other three structures is significantly lower than the prediction.

Table 3

Comparison of measured and predicted initial actuation stiffness

	S-P	**S-U**	**A-P**	**A-U**
Measured	100 N/mm	49 N/mm	42 N/mm	20 N/mm
Prediction	174.2 N/mm	87.5 N/mm	72.2 N/mm	21.8 N/mm
Ratio	0.57	0.56	0.58	0.92

6. Predicted sensitivity to manufacturing imperfections

It has already been noted that the manufacturing method gives rise to geometric imperfections in the form of misplaced nodes and bar waviness. We proceed to predict

the sensitivity of actuation stiffness to each type of imperfection, and to then compare the predicted actuation stiffnesses of the as-manufactured grids with the observed values.

6.1. Sensitivity of actuation stiffness to misplaced nodes

Recall from section 3.1 that the root mean square (RMS) value of nodal perturbation, normal to the plane of the KDLG, from that of the perfect structure equals 2.1mm. The magnitude of the imperfection of nodal location within the plane of the KDLG has been defined by the RMS value of radial displacement of each node from that of the perfect lattice; the measured RMS value for in-plane perturbation equals 0.23mm. The finite element method using the ABAQUS package is now used to predict first the effect of through-thickness nodal imperfections and second the effect of in-plane nodal imperfections upon actuation stiffness.

A MATLAB (Mathworks, 2002) routine is used to randomly displace every node of the ABAQUS input file from that of the perfect structure, for any chosen amplitude of imperfection. The finite element model uses only a single beam element for each bar and so the bars remain straight after movement of the structural nodes. Ten structural realisations were constructed by the MATLAB routine for any given amplitude of imperfection in order to gauge the scatter in actuation stiffness from one realisation to the next. The ten calculations were then used to deduce the mean and standard deviation[2].

Fig. 7a shows a plot of the mean and 95% confidence limits (± two standard deviations) of the actuation stiffness for the four 7-hexagon KDLGS versus the magnitude of nodal movement in the through-thickness direction. Likewise, Fig. 7b shows a plot of the mean and 95% confidence limits of the actuation stiffness of the four KDLGS with increasing in-plane imperfection. In both plots the RMS value of nodal imperfection has been normalised by the bar length (l = 40.5 mm).

[2] It would be preferable to perform additional simulations to give statistically significant results, but this was prohibitively time consuming.

Take the two figures together, and consider first the mean values of the responses. Out-of-plane and in-plane imperfections have only a minor effect upon the actuation stiffness for the asymmetric KDLGs, but lead to a significant drop in actuation stiffness for the symmetric KDLGs. Recall that the pin-jointed symmetric structures contain a number of internal states of self-stress which are activated by bar actuation. Geometric imperfections break the symmetry of the structure and remove these states of self-stress in the pin-jointed version. Consequently, the actuation stiffness of the rigid-jointed symmetric grids are reduced.

It is further noted from Fig. 7a and 7b that the predicted actuation stiffness displays significant scatter from one structural realisation to the next: the spread in the 95% confidence limits increases with overall magnitude of imperfection for all topologies, with the largest dispersion evident for the patched structures. Such scatter is of practical concern and suggests the need for tight quality control in manufacture.

6.2. Effect of bar waviness upon actuation stiffness

Waviness of a bar leads to a reduction in its axial stiffness and to a negligible change of bending stiffness. The relationship between the amplitude of waviness and axial stiffness of a bar can be determined straightforwardly, as follows. Consider a bar of length l, with an integral number of sine waves of waviness, of wavelength l'. Then, the misalignment w as a function of position along the bar x is

$$w(x) = w_0 \sin\left(\frac{2\pi x}{l'}\right) \tag{3}$$

where w_0 is the amplitude of waviness, as defined in Fig. 8a. Now apply an axial tension T to the ends of the bar. This tension gives rise to a bending moment M and an additional transverse displacement u such that

$$M = -EI\frac{d^2u}{dx^2} = Tw(x) \tag{4}$$

where E is the axial modulus. Substitute (3) into (4) and solve the resulting differential equation to obtain

$$u(x) = -\frac{T}{EI}\left(\frac{l'}{2\pi}\right)^2 w_0 \sin\left(\frac{2\pi x}{l'}\right) \tag{5}$$

The extension Δl of a bar with cross-section A and total length l has two contributions: the stretching of the bar and the straightening due to its initial waviness. Hence,

$$\Delta l = \frac{Tl}{EA} - \int_0^l \left[\sqrt{1+\left(\frac{du}{dx}+\frac{dw}{dx}\right)^2} - \sqrt{1+\left(\frac{dw}{dx}\right)^2}\right] dx \tag{6}$$

Upon assuming that the elastic deflection $\frac{du}{dx} << \frac{dw}{dx} << 1$ we obtain

$$\Delta l = \frac{Tl}{EA}\left(1+\frac{w_0^2 A}{2I}\right) \tag{7}$$

The axial stiffness k of the bar is therefore

$$k = \frac{T}{\Delta l} = \frac{EA}{l}\frac{1}{\left(1+\frac{1}{2}e^2\right)} \tag{8}$$

where $e \equiv w_0/\lambda$ is a non-dimensional measure of waviness given by the ratio of the amplitude of waviness w_0 to the radius of gyration of the bar cross-section λ.

The knock-down in stiffness due to bar waviness can be large. For example, consider a bar of 1mm square cross-section, and waviness of amplitude 0.6 mm. Then, e equals 2.1 and the axial stiffness of the bar is k = 0.31 *EA/l.*

It is straightforward to model the effect of bar waviness upon the bar properties within a finite element model. Recall that the effect of bar waviness is to reduce the effective axial stiffness of a bar while leaving its bending stiffness unchanged. This can be achieved by reducing the cross-sectional area of the bar by the factor $\left(1+e^2/2\right)$, while leaving the bending modulus *EI* unchanged. Finite element calculations of this type have been performed using the ABAQUS program: all bars in the KDLG are ascribed the

same level of waviness, and the actuation stiffness is determined as a function of e for each of the four variants shown in Fig. 3. It is emphasised that the nodal positions are those of the perfect structure.

Fig. 8b contains a plot of the actuation stiffness of the four KDLG variants as a function of the non-dimensional bar waviness imperfection e. The A-U KDLG is bending dominated in its performance and is largely unaffected by bar waviness. In contrast, the S-P KDLG is stretching dominated and shows a large drop in actuation stiffness with increasing bar waviness. The A-P and S-U cases are intermediate.

6.3. Comparison of predicted and measured actuation stiffness for imperfect KDLGs

It remains to match the predicted actuation stiffness for the imperfect structures and the observed actuation stiffness for the four KDLGs. Recall from Table 3 that all KDLGs except for the A-U variant have an observed actuation stiffness of 56-58% that of the perfect structure. It is clear from Fig. 7a and 7b that imperfections in nodal position (both out-of-plane and in-plane) lead to only a small drop in mean value of actuation stiffness for the symmetric KDLGs and to a negligible change for the asymmetric KDLGs. The confidence limits in Fig. 7a and 7b reveal that nodal imperfections of the magnitude observed could not give rise to the knock-down observed for three of the structures. In contrast, bar waviness is a promising candidate for the source of the reduction in actuation stiffness: it is clear from Fig. 8b that bar waviness leads to a drop in stiffness for the same three variants as that noted in Table 3. But is the agreement quantitative between predicted and measured actuation stiffness for the imperfect structures?

The predicted actuation stiffness is plotted against the measured stiffness for selected amplitudes of bar waviness in Fig. 9. It is seen that a non-dimensional amplitude of e = 1.5 (w_0 = 0.43 mm) provides reasonable agreement for all four variants of KDLG. This magnitude of waviness is in satisfactory agreement with the measured value of e = 2.0 (w_0 = 0.55 mm). It is concluded that the measured values of actuation stiffness can be explained in terms of as-manufactured bar waviness.

7. Concluding remarks

In this study, the sensitivity of the actuation performance of the Kagome Double Layer Grid (KDLG) to manufacturing defects is explored. The finite element simulations demonstrate that the observed knockdown in actuation stiffness due to imperfections is a consequence of bar waviness rather than the misplacement of nodes. It is also shown that the actuation stiffness of both the perfect and imperfect grids depend upon the detailed topology of the grids – whether symmetric or asymmetric, and whether patched or unpatched.

Insight into the differences in actuation stiffness from one variant of KDLG to the next is achieved by examining the pin-jointed parent structures. First, consider the symmetric-patched pin-jointed KDLG. In the absence of imperfections, it contains 6 states of self-stress, as detailed in Table 1. The extension of a bar by actuation triggers one or more of these states of self-stress, and the remaining structure resists actuation by the storage of elastic energy by bar stretching (and bending). The introduction of bar waviness leads to a sharp drop in the axial stiffness of the bars, and thereby to a drop in actuation stiffness, see Fig. 8b. Alternatively, an imperfection in the form of a random movement of nodes removes the states of self-stress in the pin-jointed structure, and this is reflected by a reduction in actuation stiffness of the rigid-jointed version, recall Figs. 7a and 7b.

Second, consider the asymmetric-patched KDLG. In its pin-jointed form, with one bar removed, the patched structure A-P contains a single mechanism, and can be actuated freely, with zero resistance by the surrounding structure. Random movement of nodes changes neither the number of states of self-stress (zero) nor the number of mechanisms (one), and consequently the rigid-jointed version has a negligible change in mean actuation stiffness with increasing nodal imperfection, see Figs. 7a and 7b. The moderate actuation stiffness of the rigid-jointed perfect version is due to the moderate level of stockiness of bars considered in this investigation. Consequently, the structure has some stretching resistance, and this is reduced by the introduction of bar waviness, see Fig. 8b.

Finally, consider the asymmetric-unpatched (A-U) KDLG. The perfect, pin-jointed version with one bar removed has no states of self-stress but does possess 30 mechanisms. The random movement of nodes has no effect upon the number of states of

self-stress and mechanisms, and consequently the actuation stiffness of the rigid-jointed version is insensitive to the repositioning of nodes, recall Figs. 7a and 7b. The rigid-jointed A-U KDLG deforms predominantly by bending of its constituent bars. Since the bending stiffness of a bar is almost insensitive to the presence of bar waviness the actuation stiffness is almost independent of bar waviness, as shown in Fig. 8b. The actuation stiffnesses of the perfect and imperfect A-U grid are least of all the KDLG grids investigated, due to the fact that the structure is bending dominated.

Acknowledgements

The authors are grateful for financial support from a DARPA grant on synthetic multi-functional materials and wish to thank Profs. A G Evans and J W Hutchinson for helpful discussions.

References

Babuska, I., Szabo, B.A., 1982. On the rates of convergence of the finite element method. International Journal for Numerical Methods in Engineering, 18, 323-341.

Babuska, I., Szabo, B.A., Katz, I.N., 1981. The p-version of the finite element method. SIAM Journal of Numerical Analysis, 18, 515-545.

Calladine, C.R., 1978. Buckminster Fuller's "tensegrity" structures and Clerk Maxwell's rules for the construction of stiff frames. International Journal of Solids and Structures, 14, 161-172.

Chen, C., Lu, T.J., Fleck, N.A., 1999. Effect of imperfections on the yielding of two-dimensional foams. Journal of the Mechanics and Physics of Solids, 47, 2235-2272.

Chen, C., Lu, T.J., Fleck, N.A. 2001. Effect of inclusions and holes on the stiffness and strength of honeycombs. International Journal of Mechanical Sciences, 43, 487-504.

dos Santos e Lucato, S.L., Wang. J., Maxwell, P., McMeeking, R.M., Evans, A.G. 2004. Design and demonstration of a high authority shape morphing structure. International Journal of Solids and Structures, 41, 3521-3543.

Guest, S.D., Hutchinson, J.W. 2003. On the determinancy of repetitive structures. Journal of the Mechanics and Physics of Solids, 51, 383-391.

Hutchinson, R.G., Wicks, N., Evans, A.G., Fleck, N.A., Hutchinson, J.W. 2003. Kagome plate structures for actuation. International Journal of Solids and Structures, 40, 6969-6980.

Hyun, S. and Torquato, S., 2002. Optimal and manufacturable two-dimensional, Kagomé-like cellular solids. Journal of Materials Research, 7, 137.

HKS, 2003. ABAQUS/Standard Version 6.3.1. Hibbit, Karlsson and Sorenson Inc., Providence, RI.

Leung, A.C.H., Symons D.D., Guest, S.D., 2004. Actuation of kagome lattice structures. 45th AIAA/ASME/ASCE/AHS/ASC Structures, Structural Dynamics and Materials Conference, Palm Springs, CA 19-22 April 2004.

MathWorks, 2002. MATLAB Version 6.5, The MathWorks Inc., 3 Apple Hill Drive, Natick, MA 01760-2098, USA.

Pellegrino, S. 1993. Structural computations with the singular value decomposition of the equilibrium matrix. International Journal of Solids and Structures, 30, 3025-3035.

Pellegrino, S., Calladine, C.R., 1986. Matrix analysis of statically and kinematically indeterminate frameworks. International Journal of Solids and Structures, 22, 409-428.

PTC, 2001. Pro/MECHANICA Version 23.3. Parametric Technology Corporation, Needham, MA.

Symons, D.D., Hutchinson, R.G., Fleck, N.A., 2004. Actuation performance of the Kagome Double Layer Grid. Submitted to Journal of the Mechanics and Physics of Solids.

Wicks, N., Guest, S.D., 2004. Single member actuation in large repetitive truss structures. International Journal of Solids and Structures, 41, 965-978.

Figure Captions

Fig. 1 (a) Pin-jointed, planar Kagome lattice; (b) Finite patched planar Kagome grid

Fig. 2 (a) Topology of Kagome Double Layer Grid (KDLG); (b) Modification scheme for the asymmetric KDLG with patching scheme

Fig. 3 Orthographic projections of four KDLG 7-hexagon variants: (a) symmetric-unpatched (S-U); (b) asymmetric-unpatched (A-U); (c) symmetric-patched (S-P); (d) asymmetric-patched (A-P)

Fig. 4 (a) Uniaxial stress-strain curve of low carbon steel; (b) 7-hexagon-S-U KDLG test specimen (bar length = 40.5 mm)

Fig. 5 Specimen and loading arrangement

Fig. 6 Predicted and measured load versus displacement response of (a) symmetric; (b) asymmetric KDLG specimens. The finite element predictions, labelled FE, assume finite deformations and an elastic-plastic material response.

Fig. 7 Actuation stiffness of KDLGs with (a) out-of-plane; (b) in-plane nodal imperfection (mean and 95% confidence limits). The measured actuation stiffness is given on the right-hand side for comparison.

Fig. 8 (a) Definition of bar waviness; (b) Effect of bar waviness on actuation stiffness

Fig. 9 Measured actuation stiffness of KDLG specimens plotted against predicted stiffness for bar waviness imperfection $e = 0$, 0.5, 1 and 1.5

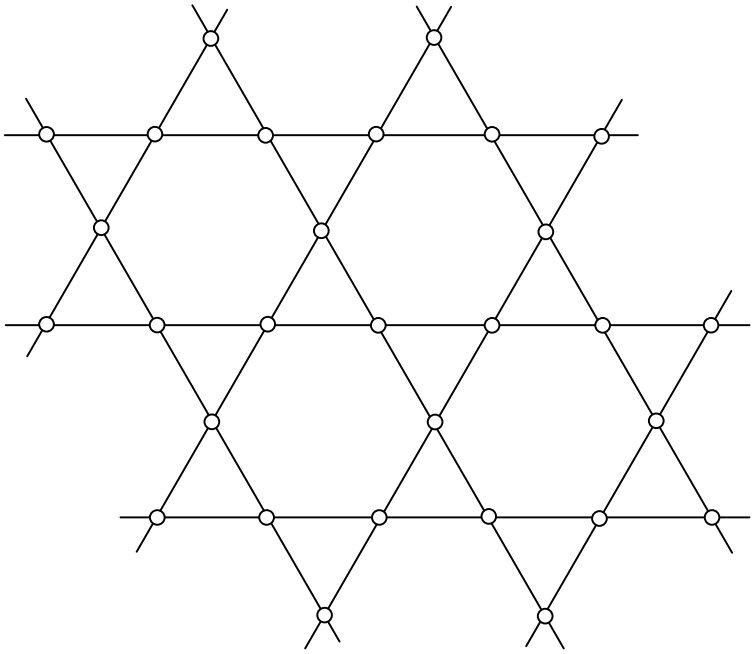

(a)

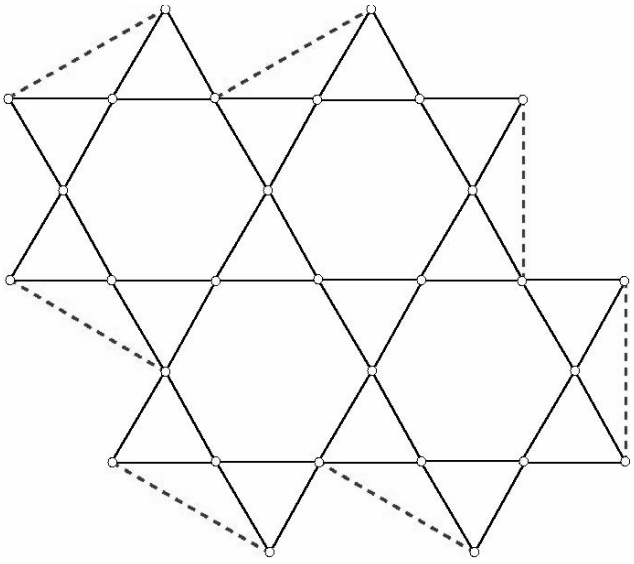

(b)

Fig. 1 (a) Pin-jointed, planar Kagome lattice; (b) Finite patched planar Kagome grid

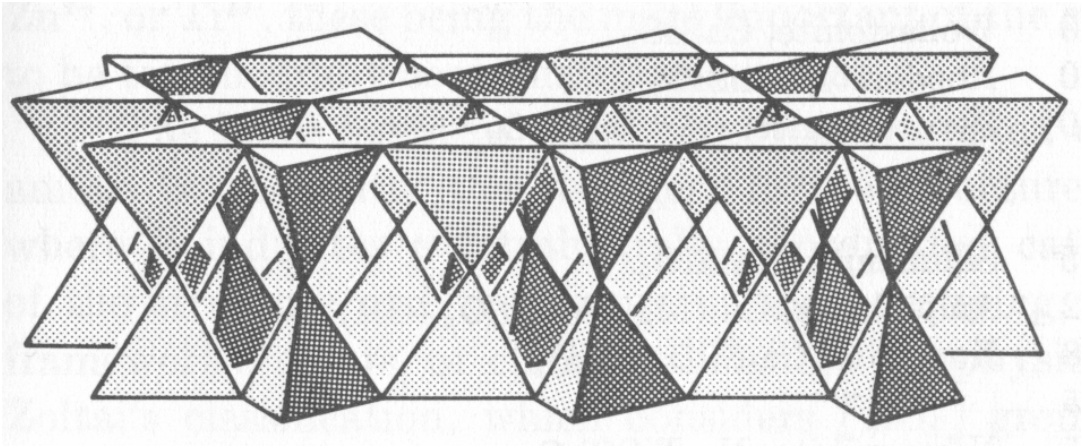

(a)

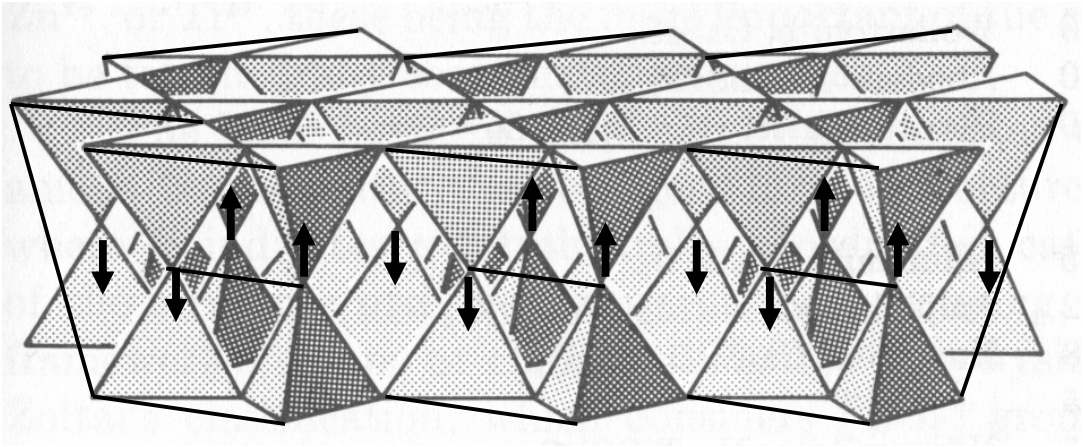

(b)

Fig. 2 (a) Topology of Kagome Double Layer Grid (KDLG); (b) Modification scheme for the asymmetric KDLG with patching scheme

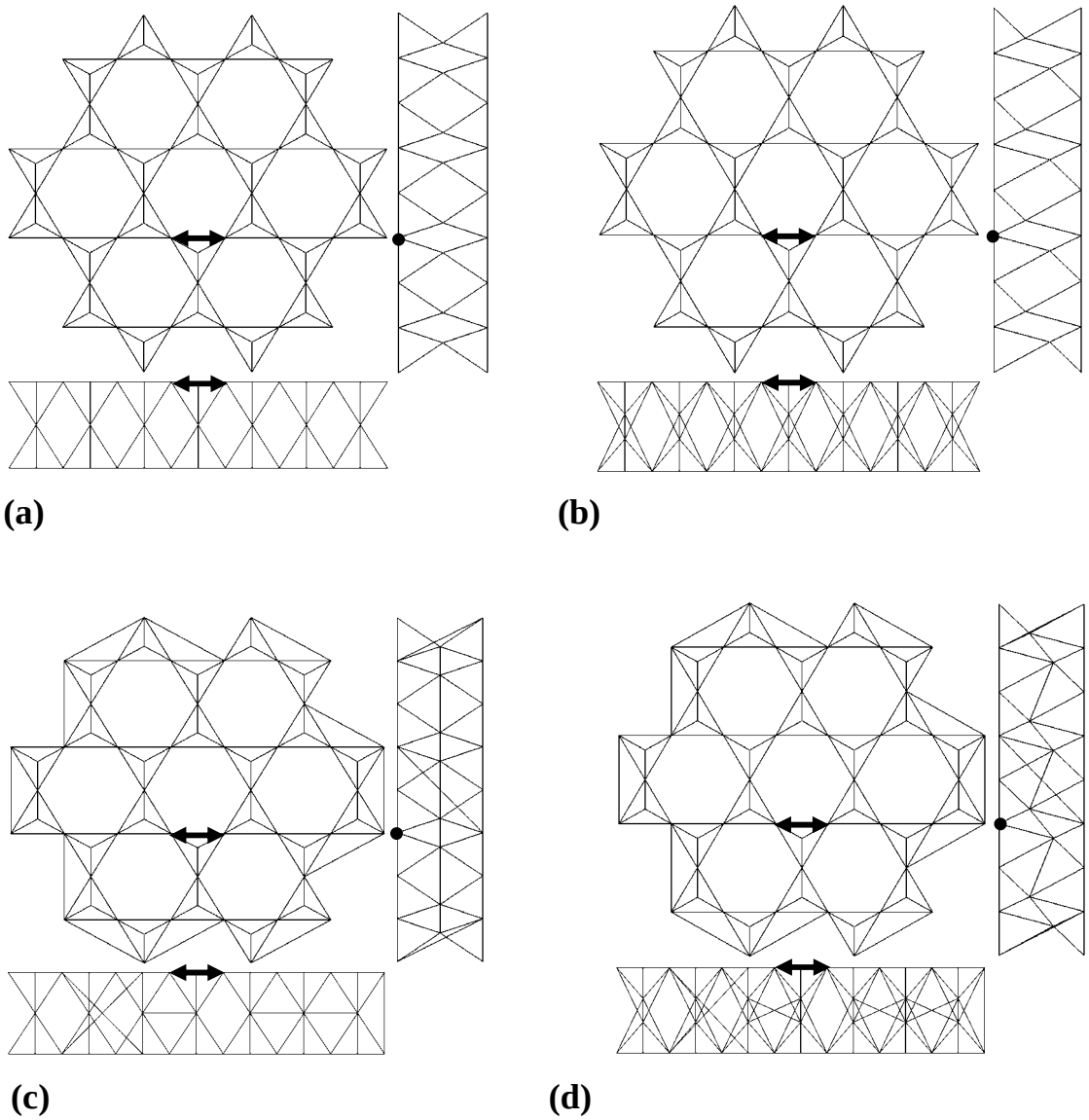

Fig. 3 Orthographic projections of four KDLG 7-hexagon variants: (a) symmetric-unpatched (S-U); (b) asymmetric-unpatched (A-U); (c) symmetric-patched (S-P); (d) asymmetric-patched (A-P)

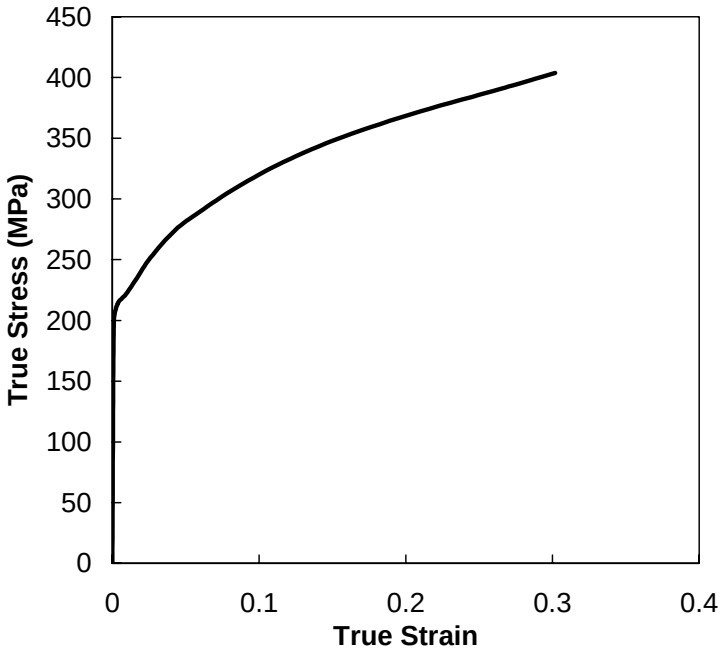

(a)

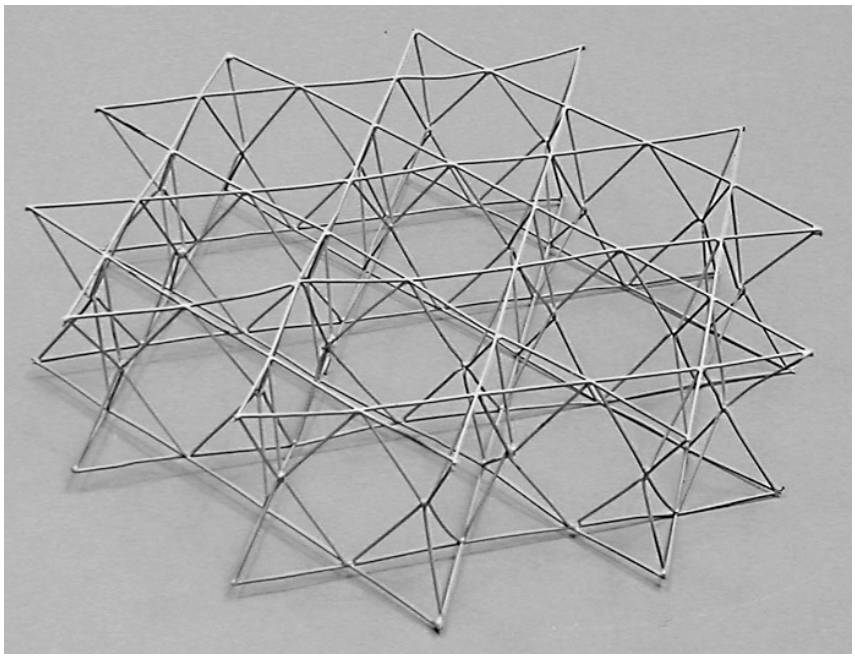

(b)

Fig. 4 (a) Uniaxial stress-strain curve of low carbon steel; (b) 7-hexagon-S-U KDLG specimen (bar length = 40.5 mm)

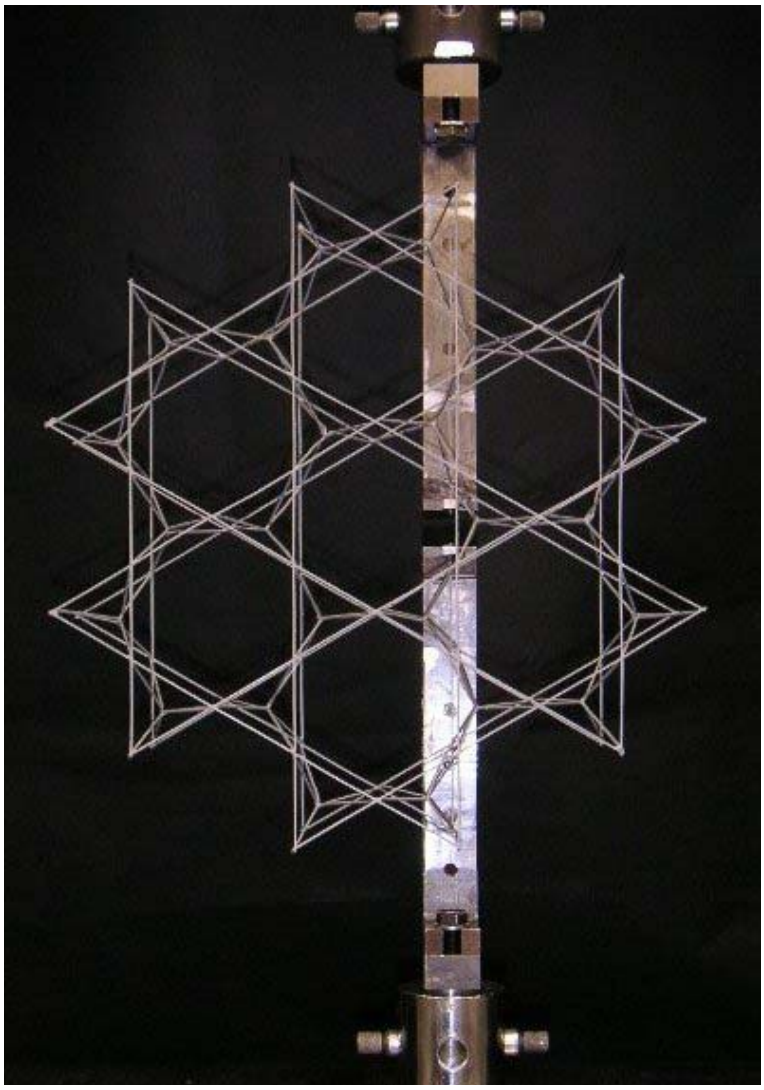

Fig. 5 Specimen and loading arrangement

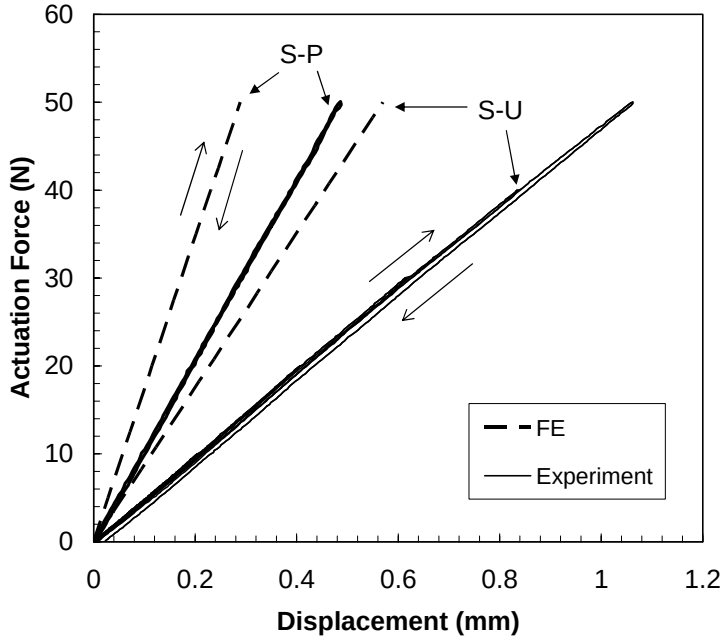

(a)

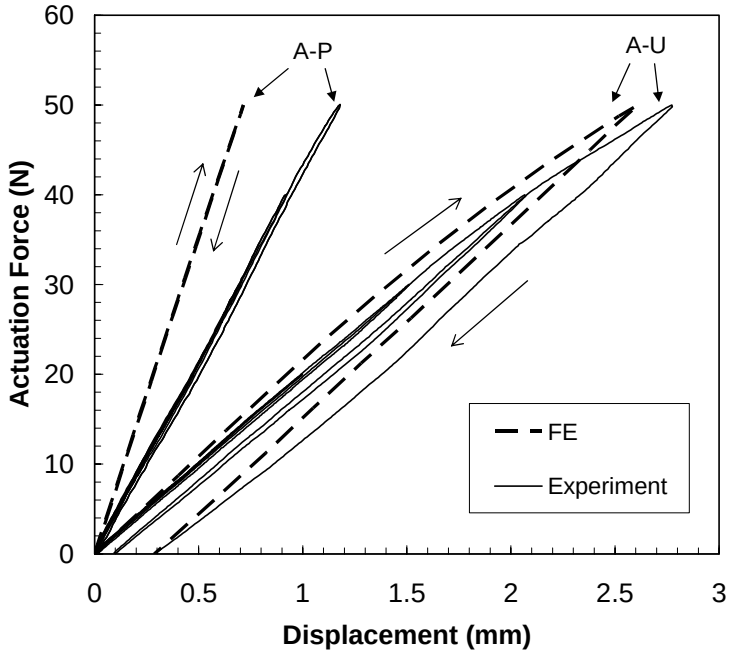

(b)

Fig. 6 Predicted and measured load versus displacement response of (a) symmetric; (b) asymmetric KDLG specimens. The finite element predictions, labelled FE, assume finite deformations and an elastic-plastic material response.

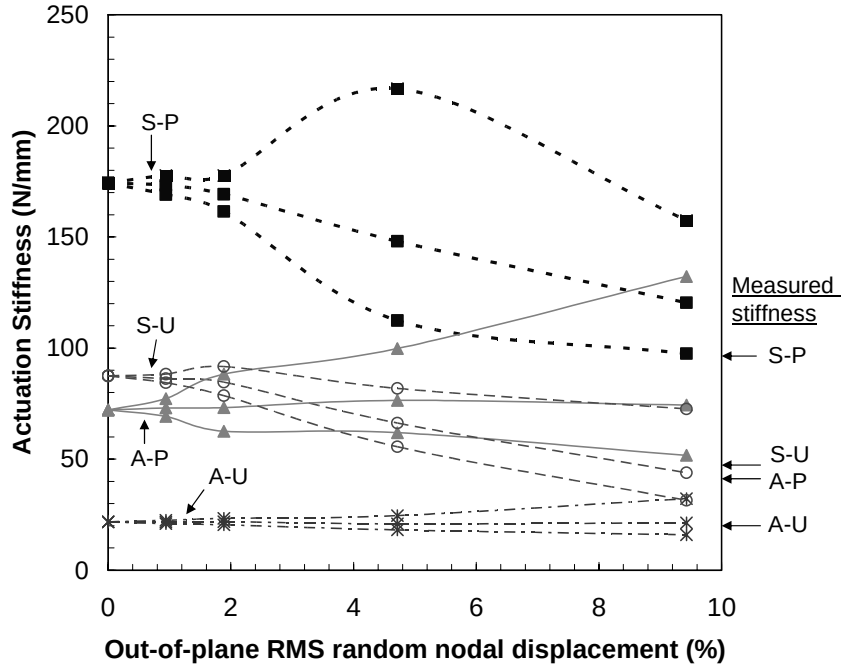

(a)

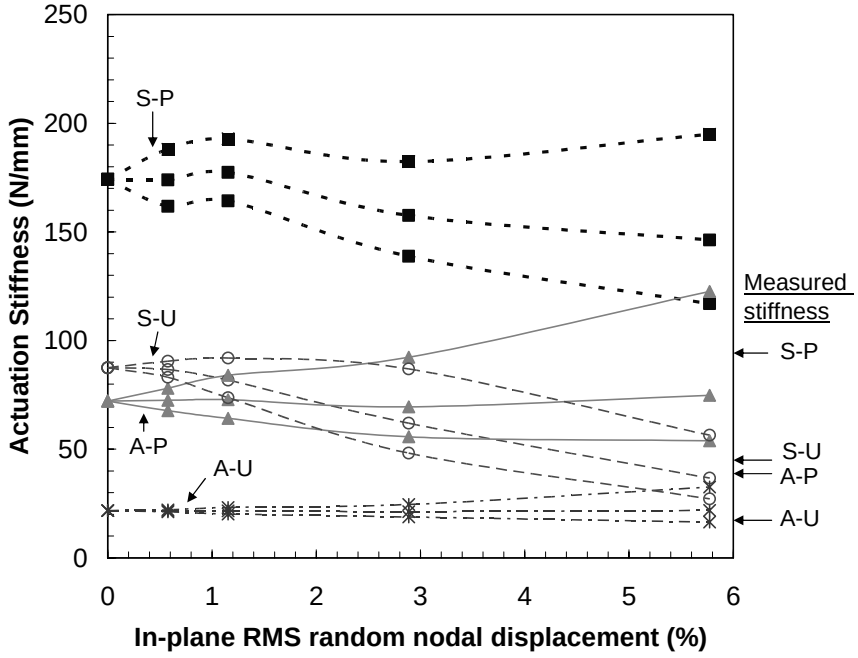

(b)

Fig. 7 Actuation stiffness of KDLGs with (a) out-of-plane; (b) in-plane nodal imperfection (mean and 95% confidence limits). The measured actuation stiffness is given on the right-hand side of the plots, for comparison.

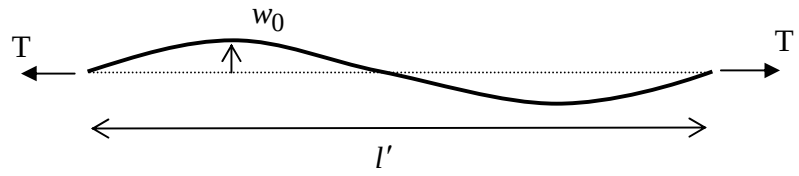

(a)

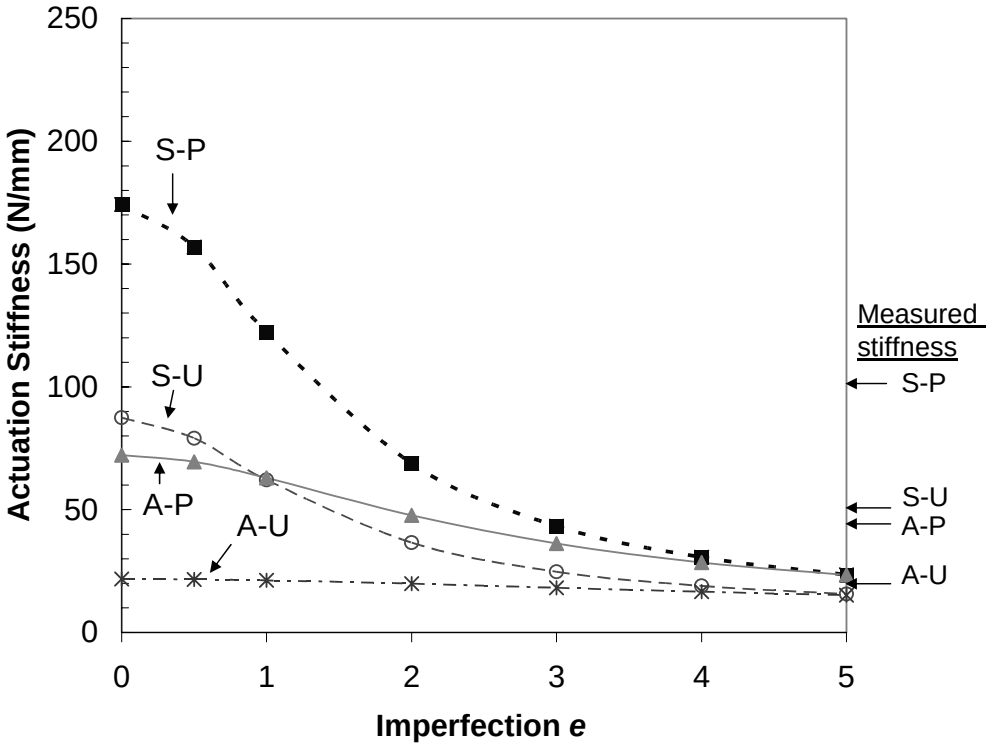

(b)

Fig. 8 (a) Definition of bar waviness; (b) Effect of bar waviness on actuation stiffness

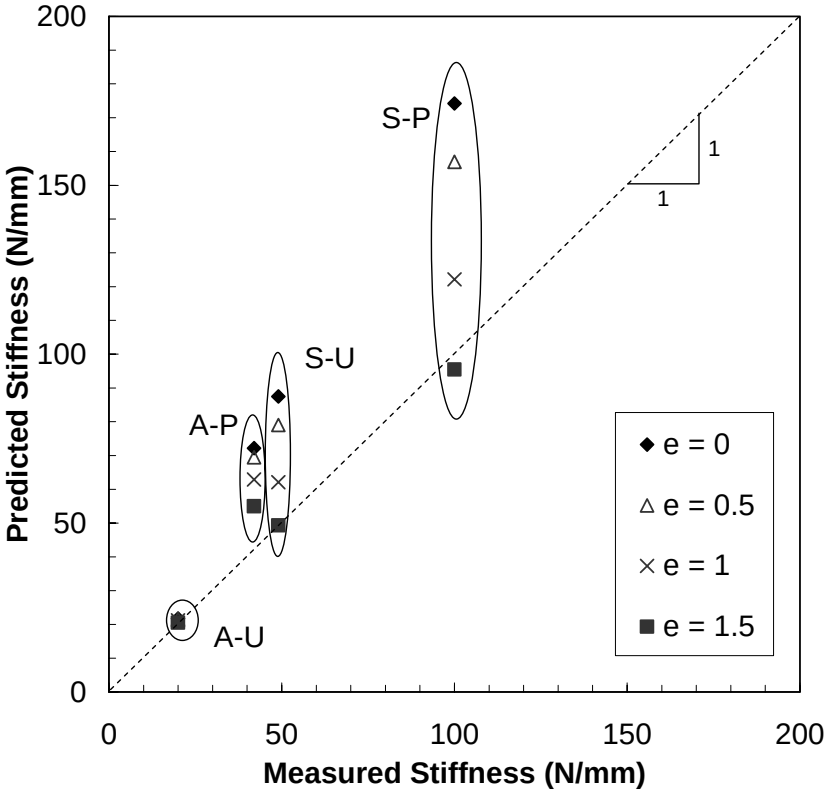

Fig. 9 Measured actuation stiffness of KDLG specimens plotted against predicted stiffness for bar waviness imperfection e = 0, 0.5, 1 and 1.5